ARMY RESEARCH LABORATORY

Indentation of Bulk Amorphous Metals to Investigate Pop-In Effects

by Tyler Krus, Thomas Juliano, and Mark VanLandingham

ARL-CR-574 **July 2006**

prepared by

Science and Engineering Apprenticeship Program (SEAP)
U.S. Army Research Laboratory

under contract

W81XWH-05-C-0058

NOTICES

Disclaimers

The findings in this report are not to be construed as an official Department of the Army position unless so designated by other authorized documents.

Citation of manufacturer's or trade names does not constitute an official endorsement or approval of the use thereof.

Destroy this report when it is no longer needed. Do not return it to the originator.

Army Research Laboratory
Aberdeen Proving Ground, MD 21005-5069

ARL-CR-574 **July 2006**

Indentation of Bulk Amorphous Metals to Investigate Pop-In Effects

Thomas Juliano and Mark VanLandingham
Weapons and Materials Research Directorate, ARL

Tyler Krus
Science and Engineering Apprenticeship Program (SEAP)

prepared by

Science and Engineering Apprenticeship Program (SEAP)
U.S. Army Research Laboratory

under contract

W81XWH-05-C-0058

REPORT DOCUMENTATION PAGE

Form Approved
OMB No. 0704-0188

1. REPORT DATE *(DD-MM-YYYY)*	2. REPORT TYPE	3. DATES COVERED (From - To)
July 2006	Final	20 June 2005–12 August 2005

4. TITLE AND SUBTITLE
Indentation of Bulk Amorphous Metals to Investigate Pop-In Effects

5a. CONTRACT NUMBER
W81XWH-05-C-0058

5b. GRANT NUMBER

5c. PROGRAM ELEMENT NUMBER

6. AUTHOR(S)
Tyler Krus,* Thomas Juliano, and Mark VanLandingham

5d. PROJECT NUMBER

5e. TASK NUMBER

5f. WORK UNIT NUMBER

7. PERFORMING ORGANIZATION NAME(S) AND ADDRESS(ES)
U.S. Army Research Laboratory
ATTN: AMSRD-ARL-WM-MA
Aberdeen Proving Ground, MD 21005-5069

8. PERFORMING ORGANIZATION REPORT NUMBER
ARL-CR-574

9. SPONSORING/MONITORING AGENCY NAME(S) AND ADDRESS(ES)
George Washington University
2121 Eye St.
Washington, DC 20052

10. SPONSOR/MONITOR'S ACRONYM(S)

11. SPONSOR/MONITOR'S REPORT NUMBER(S)

12. DISTRIBUTION/AVAILABILITY STATEMENT
Approved for public release; distribution is unlimited.

13. SUPPLEMENTARY NOTES
*Science and Engineering Apprenticeship Program (SEAP), Loch Raven High School, Baltimore, MD 21286.

14. ABSTRACT
Bulk metallic glasses (BMG) are a fairly new class of materials that exhibit high strength, low density, and corrosive resistance, as compared to traditional metals, and are useful for various applications. Spherical depth-sensing indentation of BMG reveals stepwise displacement jumps in the load-displacement curves, known as "pop-ins." These pop-ins have been found to be correlated with plastic deformation; the initial one being associated with the elastic limit of the material. The initial displacement bursts are investigated for varying stoichiometries of Zr and Hf-based BMG. Attention is focused on pressure and energy per volume at initial pop-in location as a function of different strain rates, indenter tip radius, and material composition. This research may provide further insight and understanding for macroscale behavior of BMG.

15. SUBJECT TERMS
indentation, bulk amorphous metals, mechanical testing

16. SECURITY CLASSIFICATION OF:			17. LIMITATION OF ABSTRACT	18. NUMBER OF PAGES	19a. NAME OF RESPONSIBLE PERSON
a. REPORT	b. ABSTRACT	c. THIS PAGE			Tyler Krus
UNCLASSIFIED	UNCLASSIFIED	UNCLASSIFIED	UL	22	19b. TELEPHONE NUMBER (*Include area code*) 410-306-1906

Standard Form 298 (Rev. 8/98)
Prescribed by ANSI Std. Z39.18

Contents

List of Figures

Acknowledgments

The authors are grateful to the Science and Engineering Apprenticeship Program for providing funds. Special thanks to Mr. Justin Pritchett for helping to polish the surface of the metallic glasses and to Dr. Laszlo Kecskes for assisting with SEM analysis, providing samples, and generating useful discussion.

INTENTIONALLY LEFT BLANK.

1. Introduction

Amorphous metals, otherwise known as metallic glasses, have been fervently researched since their discovery in 1960 (*1*). These materials are lightweight, exceptionally strong, and noncorrosive. In the past 15 years, material scientists have devised new bulk forms and families of metallic glasses precipitating new studies (*2*, *3*). Furthermore, reinforcement phases have improved ductility, increasing applicability in various products and calling for a better understanding of deformation behavior. To characterize mechanical behavior of these materials, tensile and compression tests have been performed, coupled with nanoindentation (*4*).

Nanoindentation has served as a significant resource in elucidating the deformation characteristics of these materials. From indentation curves, the elastic modulus, average contact pressure, energy per volume, and other parameters may be ascertained based on calculations derived from load-vs.-displacement data (*5*). With nanoindentation, a variety of stress states can be achieved, through use of different indenter tip geometries, that are both hydrostatic and deviatoric in nature. Furthermore, only small volumes of material are necessary for nanoindentation, which allow for investigating microscale material failure mechanisms and finding local variation of properties.

Recent research using nanoindentation has provided insights on nucleation kinetics and mode of plasticity for bulk metallic glasses (BMG) (*6*, *7*). Transmission electron microscopy of the indentations *ex situ* unveiled that recrystallization occurs without heating during quasistatic loading conditions. However, the nucleation kinetics' driving force remains unclear. Further, nanoindentation studies have shown that lower loading rates exhibit more serrated flow than higher loading rates for sharp indenter geometries (*6*). It has been shown that slower loading rates cause BMG to exhibit individual shear bands, while in higher loading conditions, shear bands operate at the same instant creating the appearance of a more uniform deformation behavior (*6*). However, studies thus far have failed to consider the pressure conditions or energy per volume at the initial pop-in location signifying the initial point of plastic failure. The focus of this study is to use nanoindentation to understand the point of initial plastic deformation when strain rates, stoichiometry, and indenter tip radius are varied. It is anticipated that extrapolation of loading conditions and energy absorption per volume into the macroscale will guide understanding of failure conditions across various applications.

2. Experimental Setup

The BMG used in this study were 3-mm-diameter cylindrical ingots mounted in epoxy that had compositions of $(Hf_xZr_{1-x})_{52.5}Ti_5Ni_{14.6}Cu_{17.9}Al_{10}$, where "x" was either 0 (20), 0.4 (22), or

1.0 (25). Numbers in parenthesis indicate the corresponding sample designation for the different compositions. X-ray diffraction indicated that the glasses were amorphous except for small crystallization peaks in metallic glasses 20 and 25, or the Zr and Hf rich samples, respectively. In order to ensure repeatable indentation results, sample surfaces were polished with diamond paste to a mirror finish. Finally, the backside of each sample was ground until the BMG was exposed at the surface and this piece was in turn glued to a stiff aluminum puck. This was done to eliminate compliance effects from the epoxy mount.

The indentation experiments were conducted using a Nano Indenter XP (MTS Systems), which measures load and displacement continually through the duration of the loading and unloading cycle. This machine can apply loads of up to 733 mN and has a total displacement range of 1.5 mm. Experimental resolution of measurement has been typically found to be around 10 μN and 0.1 nm for load and displacement, respectively. Before each indentation, the thermal/electronic drift rate of the indenter resting on the surface was measured to be below 0.05 nm/s. To create markedly different stress states underneath the indenter, the three diamond tips used for indentation had a spheroconical geometry with a nominal radius of either 3, 20, or 50 μm. Indentation strain rates (loading rate divided by load) of 0.1, 0.05, and 0.01 1/s were used for each indenter geometry. Each BMG was tested with each tip under each loading rate. For each condition, the maximum applied load was held for either 0 or 10 s and unloading took place over 10 s. Figure 1 illustrates a common profile for applied load with time. After indentation, selective BMG indents were examined using a Hitachi S4700 field emission scanning electron microscope (SEM).

For each condition, a 5 × 5 array was indented 1000 nm into the surface to ensure at least one pop-in, and a 3 × 3 array at a more shallow depth was used to verify purely elastic behavior prior to pop-ins. To determine the location of a displacement burst, at least two elastic curves were superimposed on the load-vs.-displacement results providing visible deviations from the curve. In cases where the displacement burst was unusual or difficult to detect, the curve was not considered in the analysis. If the pop-in event was difficult to detect, the method developed by Juliano et al. (*8*) was used to determine event locations based on the derivative of the load-vs.-displacement graph. The maximum difference in sequential data points that did not indicate a pop-in event was determined by the derivative of the elastic curves' greatest fluctuation between successive data points. In each indeterminable curve, if a difference was greater than the greatest of the elastic curves, the displacement location of the initial data point was noted and established as the initial point of pop-in behavior. The first instance of this effect in a given curve was the only value established as a primary pop-in.

Energy-per-unit volume and contact pressure were calculated in the following manner. Energy was taken as the area underneath the load-displacement curve, as determined by the Testworks 4 software (MTS Systems). The total elastically deformed volume was defined as the volume of the indenter displaced into the original surface. This assumption necessitates that the material is

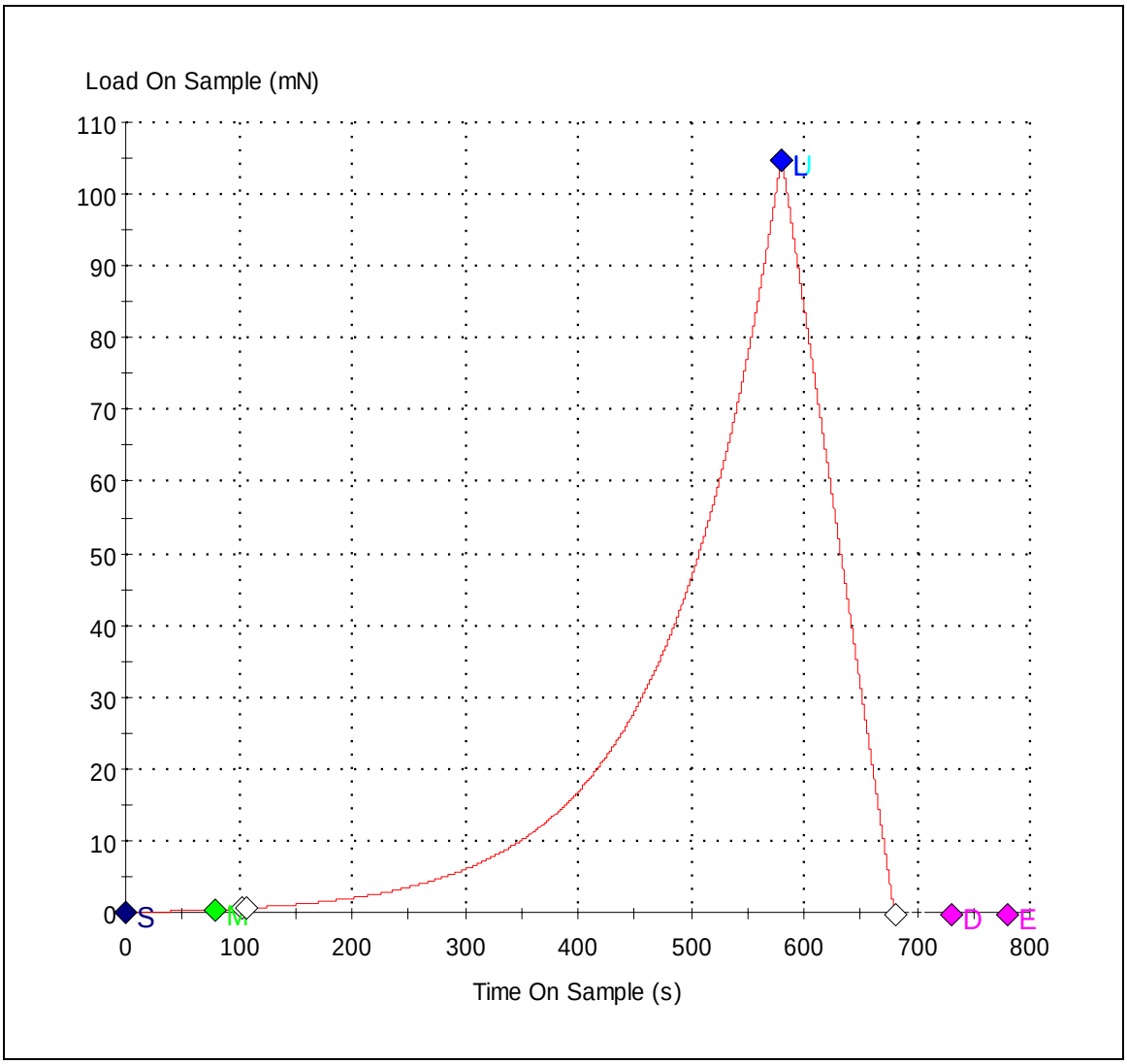

Figure 1. Typical indentation loading profile as a function of time.

incompressible, which is not the case since Poisson's ratio for these BMG is ~0.3 and not 0.5. It is admitted that this assumption will introduce some error into the measurement methodology; however, no better option could be conceived at this time. Volume was computed by integration of area coefficients calibrated from fused-silica indentation data, with the point of contact and total displacement used as evaluation boundaries. Due to the difficulty of calibrating an accurate description of tip geometry at shallow depths (<100 nm), energy per volume could not be considered for the 3-µm-radius spherical tip because of the shallow initial pop-in location. Contact pressure at the location of the pop-in was taken to be the ratio of the applied load to the contact area, as determined by calibration of area coefficients for each indenter.

3. Results and Analysis

From the data collected and shown in figure 2, it is seen that Hf-based BMG generally fail at greater pressure and energy per volume than the Zr-based BMG, based on the initial point of pop-in. Furthermore, Hf-based BMG is more sensitive to indenter tip radius in regards to both pressure and energy per volume at initial failure.

Larger radius spheres required greater energy per volume, but less pressure to pop-in for similar indentation conditions. This could be justified by taking into account the time-dependent nature of the material. For smaller radius spheres, pressure is generated much more quickly during the initial displacement into the surface. This is illustrated in the experimental data shown in figure 3. Because BMG is time dependent (*4*), the greater pressure required to pop-in is a direct result of the material being able to withstand greater pressure for a short amount of time. Decreasing indentation strain rate in previous research has shown a tendency toward more serrated flow (*4*). Furthermore, in this work pop-ins could occur during the hold at peak load (figure 4) and a few that actually exhibited this effect during unloading (see figure 5).

To explain energy-per-volume trends, the actual indenter tip geometry must be considered. The 50-μm nominal radius sphere tip geometry initially has a smaller radius (~20 μm) at depths below ~200 nm that grows into a larger radius (~50 μm) while the opposite was true for the 20-μm tip. This was determined by measuring the tip geometry with atomic-force microscopy as well as calibration with fused silica. As a result, there would be less and more actual displaced volume for the 50- and 20-μm nominal radius tips, respectively, compared to a perfect sphere. This does not affect pressure as significantly because it is evaluated past this point of transition in geometry and computed at a single location. Energy per volume, on the other hand, takes into account the history of contact area throughout the indentation.

Even though BMG are known to be loading-rate sensitive, the range of strain rates used in this study do not appear to affect either pop-in pressures or energy per volume at the point of pop-in. However, load-displacement behavior was markedly different between the three different radius indenters. When using the 3-μm-radius sphere at loads above 150 mN, a regular stepwise pattern was found in the load-displacement curves (see figure 6). This pattern was more pronounced in the slower strain rate loading conditions. This fluctuated between periods of pop-ins and elastic behavior at a constant rate. It is possible that this effect was not observed for the 20- and 50-μm-radius spheres because depths significant enough to generate similar pressure states were not obtained. Under large enough contact pressures (~9.5 GPa), for a spherical geometry, pop-in behavior becomes much more predictable and regular than for sub-critical values.

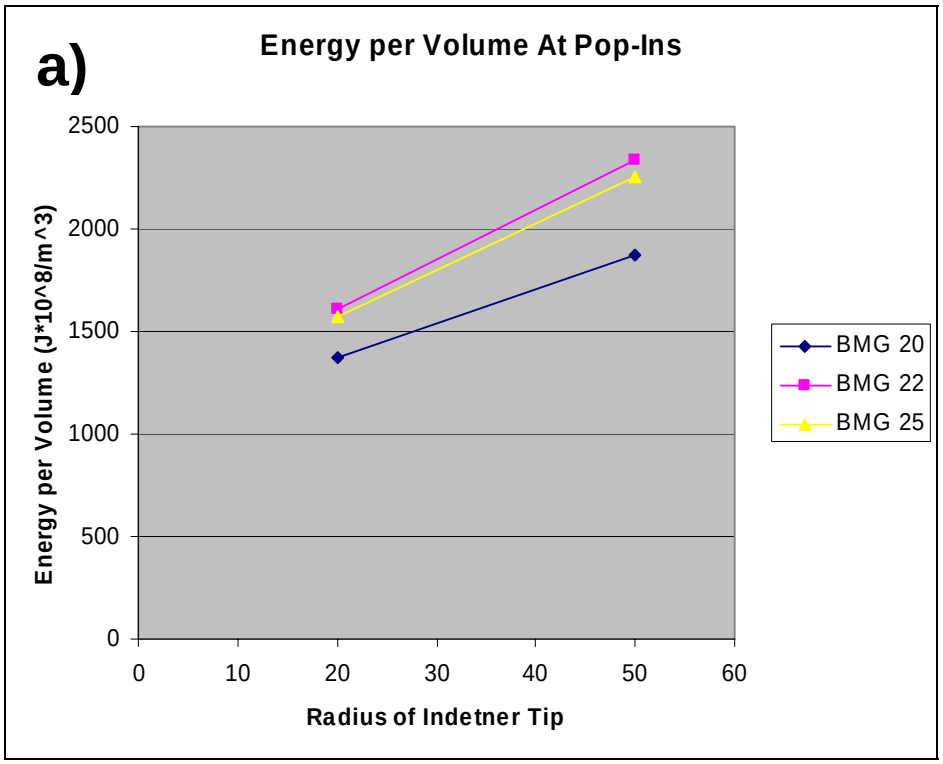

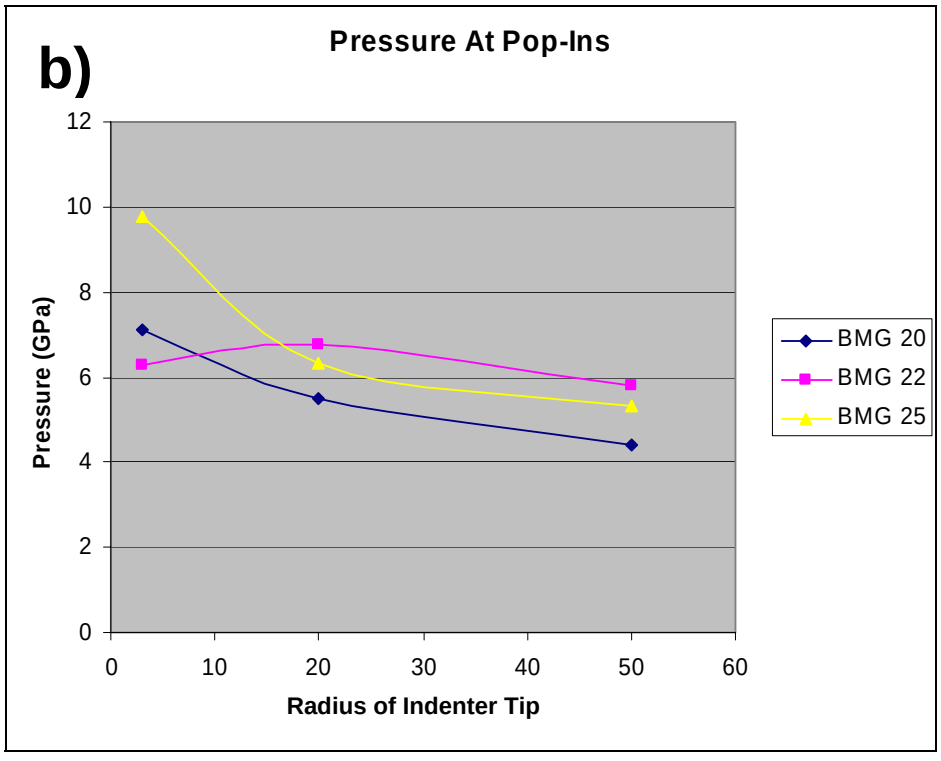

Figure 2. Comparison of Zr-based and Hf-based energy per volume (a) and pressure at pop-in locations (b) as a function of radii.

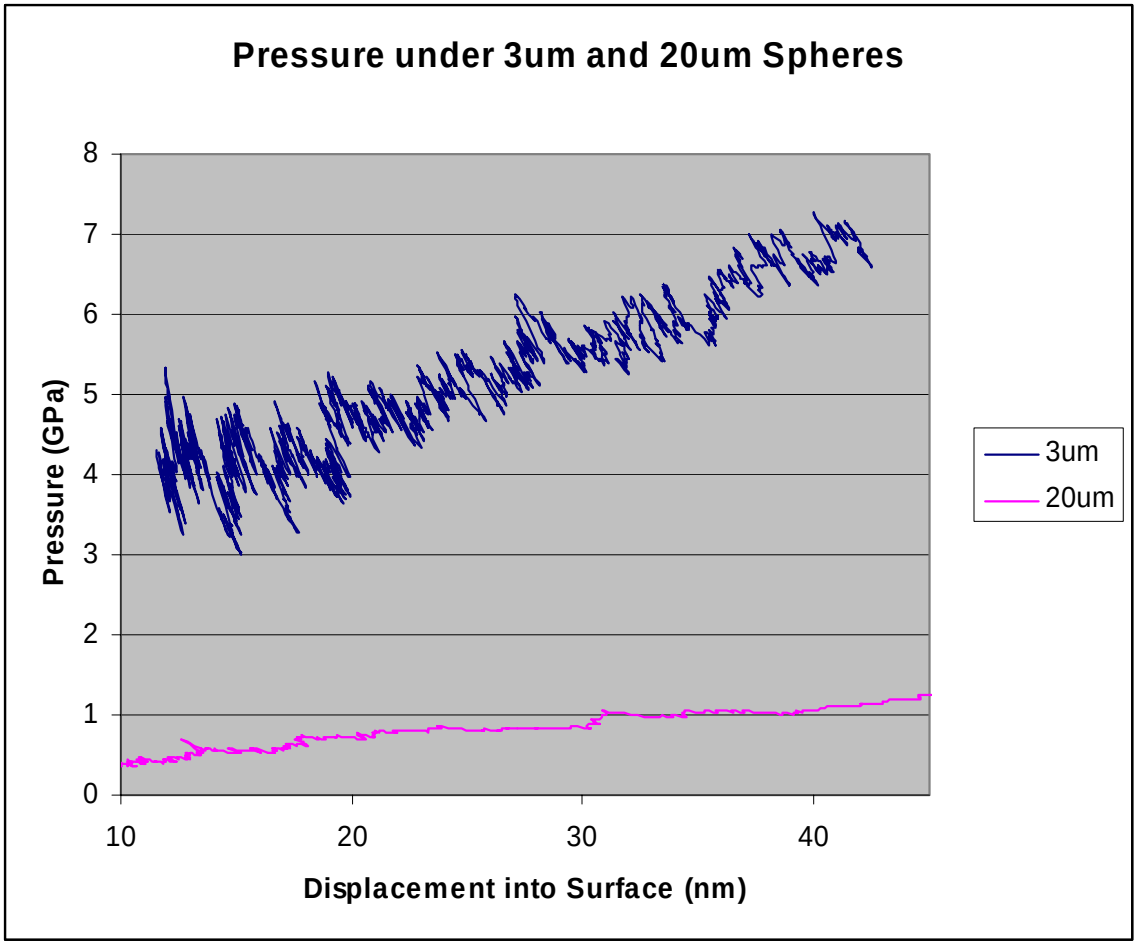

Figure 3. Pressure generated for a 3-µm (upper) and 20-µm (lower) radius sphere as a function of displacement into the surface.

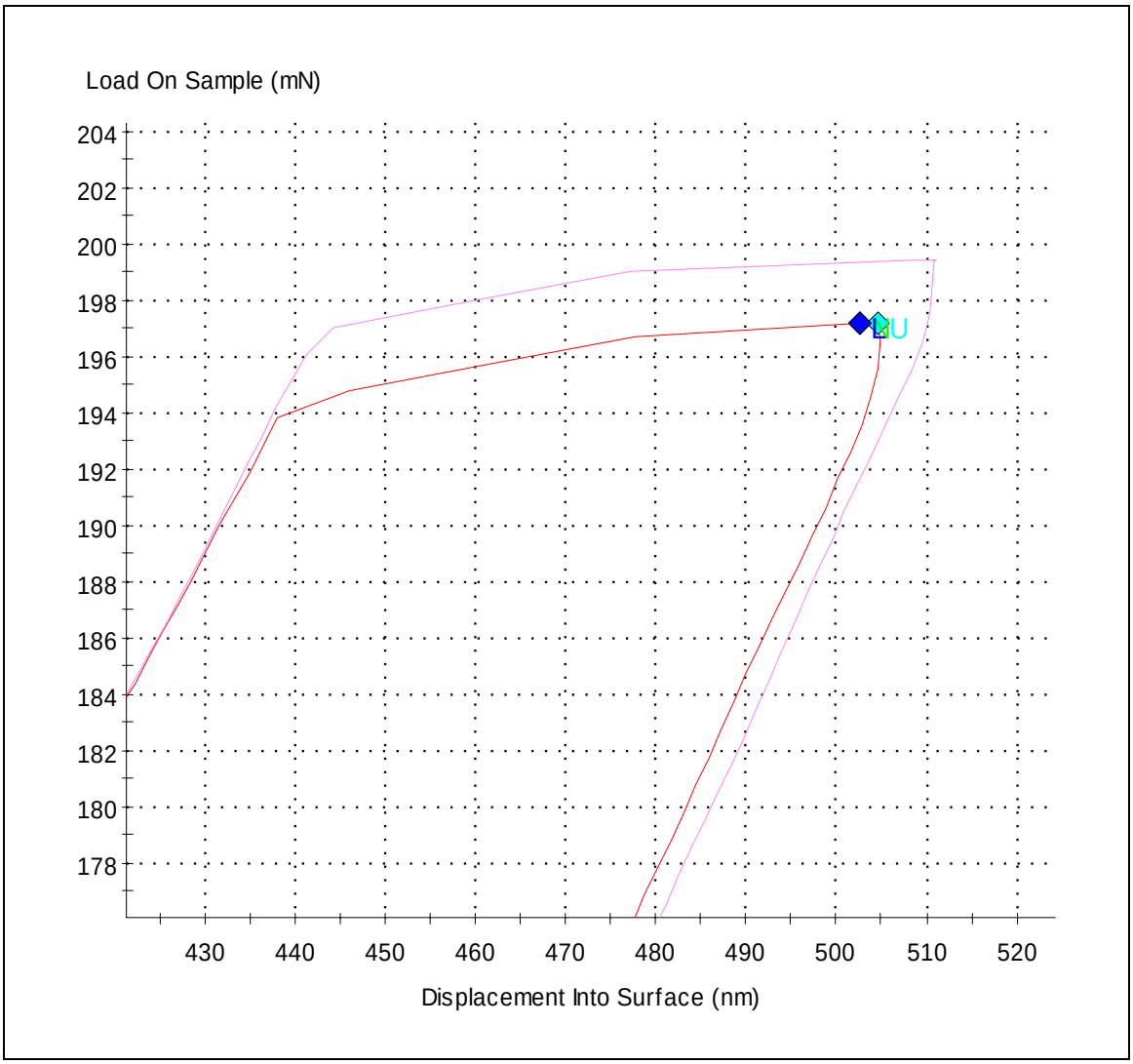

Figure 4. Pop-ins that occur at peak load.

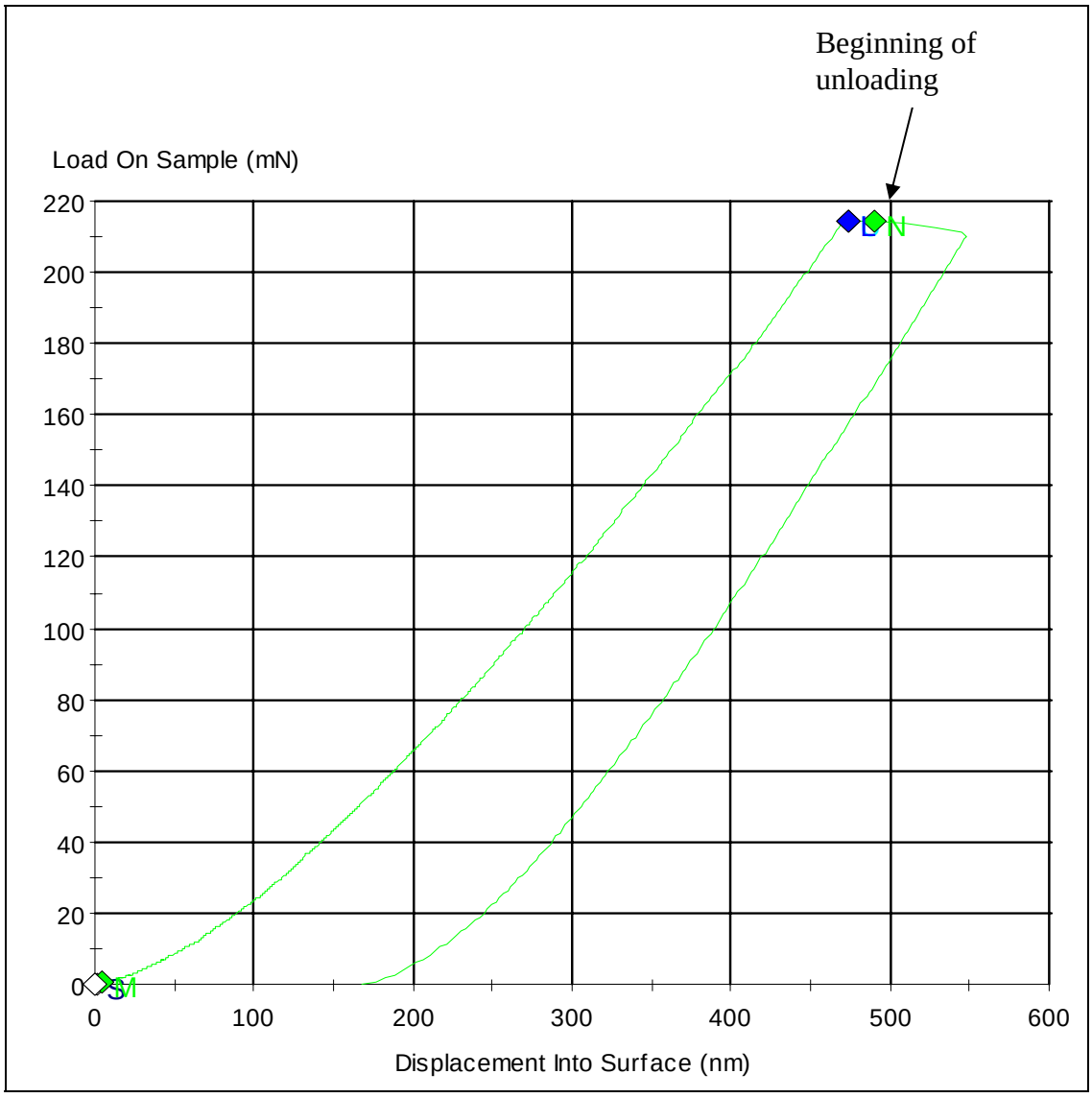

Figure 5. Pop-in that occurs during unloading segment.

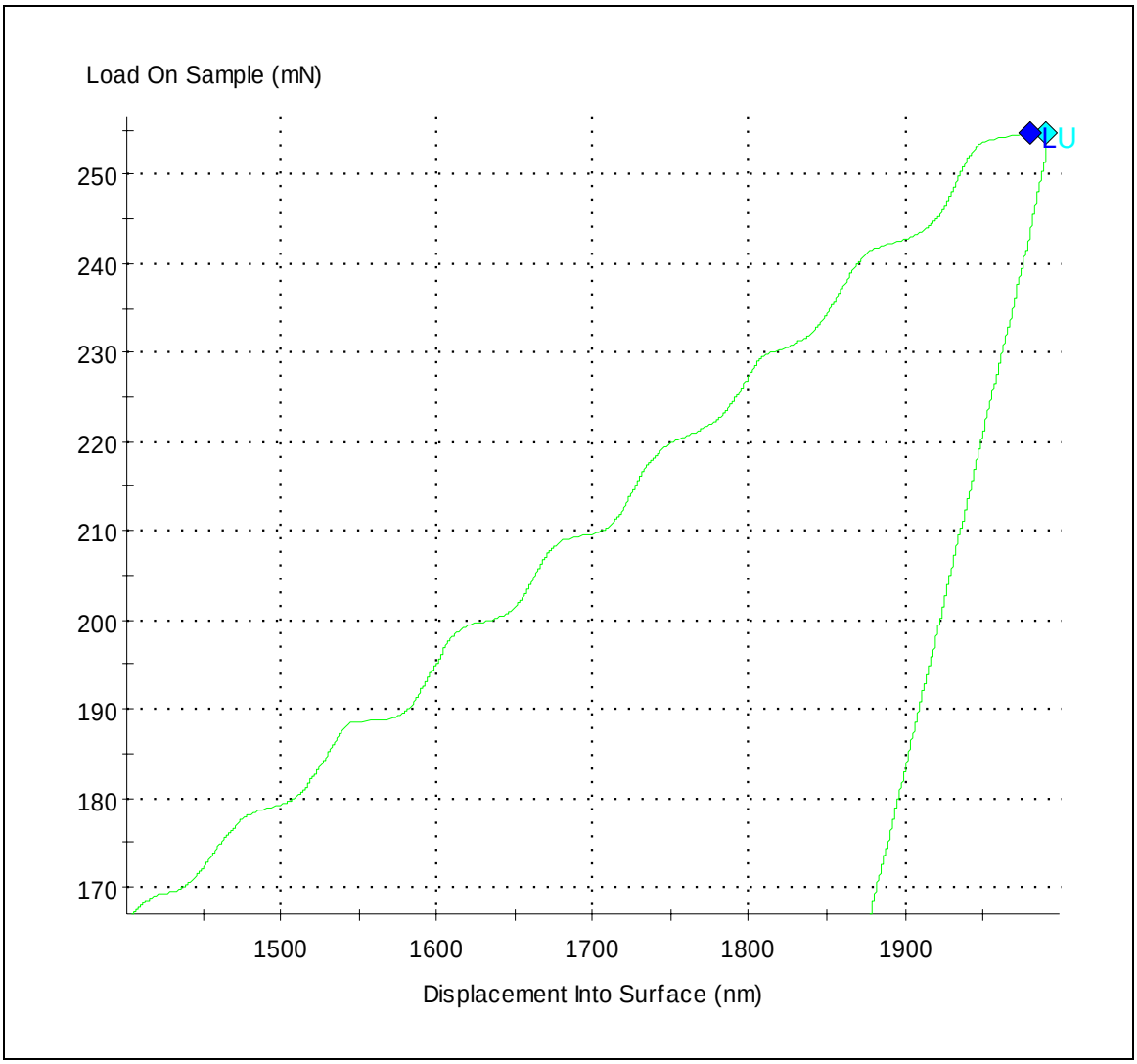

Figure 6. Stepwise pattern exhibited in excess of 150 mN for indentation of 3-µm sphere.

After indentation, SEM qualified that shear banding occurred underneath the surface under various indent locations, with a 3-μm-radius indenter indent shown in figure 7. Bands could be found most noticeably under these conditions, around the perimeter of the indent. Furthermore, residual imprints of slower strain rates were often deeper, signifying that more plasticity and a greater displacement from pop-ins occurred under slower conditions.

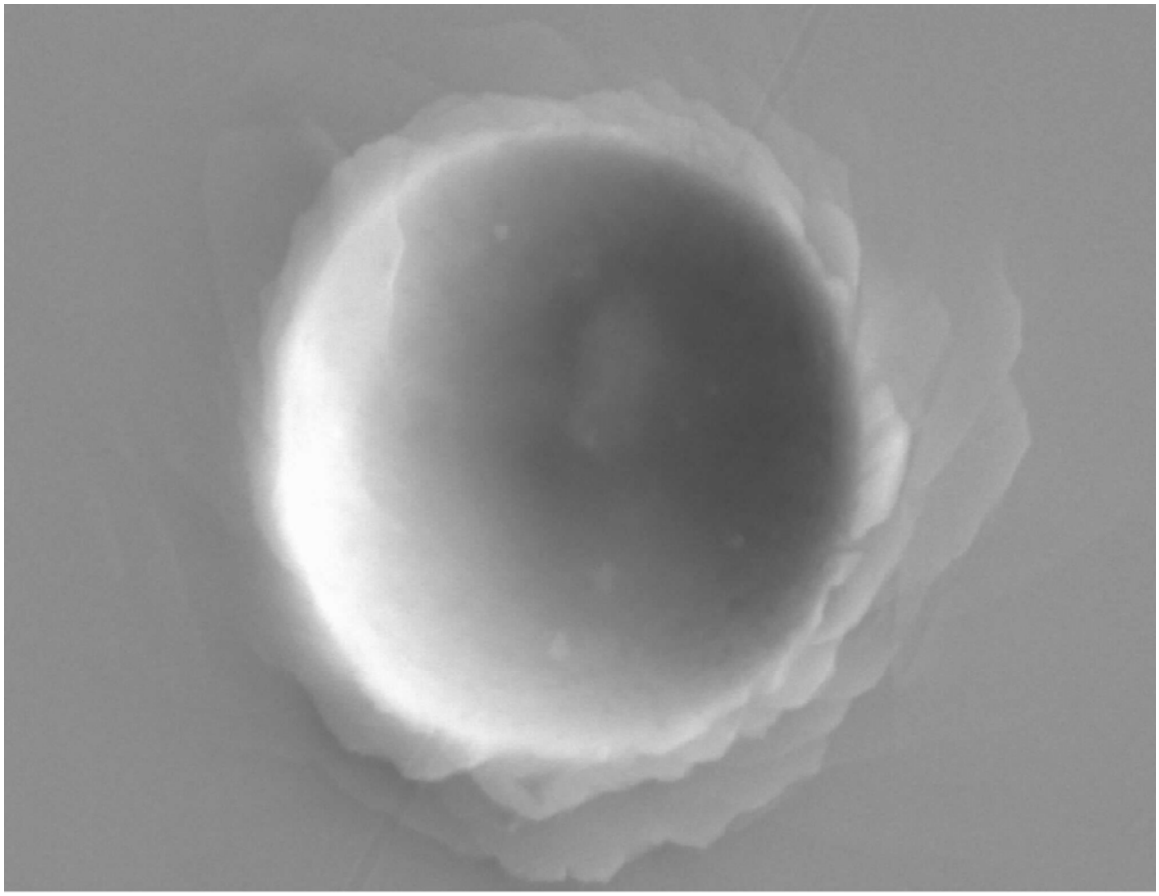

Figure 7. SEM micrograph of an indentation made by the 3-μm-radius indenter. Clear effects of subsurface shear bands can be seen on the surface of the indented area.

4. Conclusions

A number of indentation tests were performed under various conditions on BMG samples and the following conclusions can be made: (1) Zr-based BMG was found to initially fail at lower contact pressures than Hf-based BMG. (2) Indentation strain rate was shown to have little effect for rates of 0.01 to 0.1 1/s. (3) Increasing the radius of the indenter tip appears to lower the pressure and to increase energy per volume necessary for a pop-in to occur.

Further research should be guided into understanding if greater magnitude changes in strain rate generate unique points of pop-in in regards to pressure and energy per volume. The time dependence of this material is essential for an understanding of it. Research on the effect of holding at the peak load, the nature of the stepwise pop-ins above pressures above 9.5 GPa, and pop-ins on unloading curves would be beneficial to further understanding of BMG.

5. References

1. Klement, W.; Willens, R.; Duwez, P. *Nature* **1960**, *187*, 869.
2. Johnson, W. *Journal of Mechanics* **2002**, *54*, 40.
3. Li, J. *Treatises in Materials Science* **1981**, *20*, 325.
4. Schuh, C.; Neih, T. *Journal of Materials Research* **2003**, *19*, 1.
5. Fischer-Cripps, A. *Nanoindentation*; Springer: New York, 2004.
6. Schuh, C.; Argon, A.; Nieh, T.; Wadsworth, J. *Philosophical Magazine A* **2003**, *83*, 2585.
7. Jiang, W.; Pinkerton, F.; Atzmon, M. *Journal of Applied Physics* **2003**, *93*, 9287.
8. Juliano, T.; Domnich, V.; Buchheit, T.; Gogotsi, Y. *Proceedings of the Materials Research Society Symposium, 791*, 2004, pp Q7.5.1-Q7.5.11.

NO. OF
COPIES ORGANIZATION

1 (PDF ONLY) DEFENSE TECHNICAL INFORMATION CTR
DTIC OCA
8725 JOHN J KINGMAN RD
STE 0944
FORT BELVOIR VA 22060-6218

1 US ARMY RSRCH DEV & ENGRG CMD
SYSTEMS OF SYSTEMS INTEGRATION
AMSRD SS T
6000 6TH ST STE 100
FORT BELVOIR VA 22060-5608

1 INST FOR ADVNCD TCHNLGY
THE UNIV OF TEXAS
AT AUSTIN
4030-2 W BRAKER LN
AUSTIN TX 78759-5329

1 DIRECTOR
US ARMY RESEARCH LAB
IMNE ALC IMS
2800 POWDER MILL RD
ADELPHI MD 20783-1197

3 DIRECTOR
US ARMY RESEARCH LAB
AMSRD ARL CI OK TL
2800 POWDER MILL RD
ADELPHI MD 20783-1197

3 DIRECTOR
US ARMY RESEARCH LAB
AMSRD ARL CS IS T
2800 POWDER MILL RD
ADELPHI MD 20783-1197

ABERDEEN PROVING GROUND

1 DIR USARL
AMSRD ARL CI OK TP (BLDG 4600)

NO. OF
COPIES ORGANIZATION

ABERDEEN PROVING GROUND

8 DIR USARL
AMSRD ARL WM
J MCCAULEY
AMSRD ARL WM MA
M VANLANDINGHAM
T JULIANO (4 CPS)
AMSRD ARL WM MB
L KECSKES
R DOWDING